Journal of Applied Polymer Science

Poly(propylene carbonate)/aluminum flake composite films with enhanced gas barrier properties

Lipeng Zhai,[1] Gaofeng Li,[1] Yan Xu,[2] Min Xiao,[1] Shuanjin Wang,[1] Yuezhong Meng[1]

[1]State Key Laboratory of Optoelectronic Materials and Technologies/The Key Laboratory of Low-Carbon Chemistry & Energy Conservation of Guangdong Province, Sun Yat-sen University, Guangzhou 510275, People's Republic of China

[2]Instrumental Analysis & Research Center, Sun Yat-sen University, Guangzhou 510275, People's Republic of China

Correspondence to: Y. Z. Meng (E-mail: mengyzh@mail.sysu.edu.cn) and Y. Xu (E-mail: xuyan@mail.sysu.edu.cn)

ABSTRACT: A series of poly(propylene carbonate) (PPC)/aluminum flake (ALF) composite films with different ALF contents were prepared via a melt-blending method. Their cross-section morphologies, thermal properties, tensile strength (TS), and gas barrier properties were investigated as a function of ALF contents. SEM images reveal the good dispersion and orientation of ALF along with melt flow direction within PPC matrix. The oxygen permeability coefficient (OP) and water vapor permeability coefficient (WVP) of the composite films decrease continuously with ALF contents increasing up to 5 wt %, which are 32.4% and 75.2% that of pure PPC, respectively. Furthermore, the TS and thermal properties of PPC/ALF composite film are also improved by the incorporation of ALF particles. The PPC/ALF composite films have potential applications in packaging area due to its environmental-friendly properties, superior water vapor, and oxygen barrier characteristics. © 2014 Wiley Periodicals, Inc. J. Appl. Polym. Sci. **2015**, *132*, 41663.

KEYWORDS: biodegradable; blends; composites; manufacturing; packaging

Received 19 May 2014; accepted 20 October 2014
DOI: 10.1002/app.41663

INTRODUCTION

The white pollution caused by petroleum-based materials has become an international environmental issue and the limited petroleum has driven amount of efforts to explore biodegradable or bio-based materials.[1,2] Additionally, global warming, also known as the greenhouse effect, is caused by the mass emission of CO_2 produced by industries.[3–5] Therefore, the fixation of carbon dioxide has attracted a great deal of interest as a means to reduce greenhouse gas pollution and has been considered an alternative to overcome shortages in conventional petroleum fuel supplies. In these regard, much attention has been paid to the synthesis of degradable aliphatic polycarbonates from carbon dioxide since the pioneering work by Inoue.[6–13]

Poly(propylene carbonate) (PPC) is one of these aliphatic polycarbonates that has been extensively studied and its production is known to have been industrialized.[14–16] The resulting PPC exhibits an alternating molecular structure as illustrated in Figure 1, and it also showed superior mechanical properties and considerable degradability in both soil and buffer. Importantly, PPC synthesis recycles carbon dioxide from the environment and has meaningful chemical and physical properties such as compatibility, impact resistance, high translucence, and innocuousness. Such properties are advantageous in adhesives, plasticizers, solid electrolytes, barrier materials, and new materials for packaging applications.[17]

Recently, to expand the application of PPC, great efforts have been devoted to improve the deficient thermal, mechanical, and barrier properties of PPC, including the chemically modifying the end group[18] and the physical method such as blending it with other polymers[19,20] or introducing inorganic fillers.[21,22] Among these methods, addition of various types of fillers is commercially advantageous as the physical properties are readily manipulated by the type and concentration of fillers.[23] However, for conventional filler/PPC composites, the high loading level of fillers causes the deterioration of some properties, such as the high density and the loss of toughness. Thus, it is still a challenging work to obtain PPC composites with superior thermal, mechanical, barrier, and processing properties with quite low filler content.

High aspect ratio flakes or platelets have been used to enhance gas barrier properties of polymers.[24] Platelet-type fillers such as aluminum flake (ALF), mica, and talc are most useful in thin barrier films.[25] Besides, for packaging materials, the best barriers can be achieved with laminates incorporating metallized films. Aluminum layers about 50–80 nm thick allow very low gas transmission rates (O_2 TR, 0.02 cm^3 m^{-2} day^{-1}; water vapor

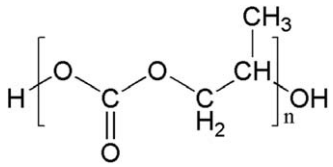

Figure 1. Structure of PPC.

TR, 0.05 g m^{-2} day^{-1}). Therefore, A1 metallization is now currently used and provides most of the properties required: barrier, restorability, flexibility, cost.[26] Nowadays, aluminized polypropylene and polyester films are widely used as gas barrier materials in a variety of food and medical packaging applications.[27]

To our knowledge, there has been no report on PPC/ALF composite films and their properties for use as packaging materials. Herein in this work, we report the preparation of PPC/ALF composites in order to improve the comprehensive performances of PPC-based composites. Five different PPC/ALF composite films were prepared via melt blending, and the effects of the ALF content on the oxygen permeability, water permeability, morphological structure, thermal properties, and mechanical properties of the films were investigated.

EXPERIMENTAL

Materials

Industrial grade PPC [melt flow rate (MFR) (190°C, 2.16 kg) = 8.6 g/10 min], with a number-average molecular weight (M_n) of 80,000 Da and a polydispersity (PD) of 1.9, was supplied by Tianguan Enterprise Group (Henan, China). Aluminum flake with an average size of 3–5 μm were supplied by Zuxing AT Co. (Shenzhen, China). All above materials were dried in a vacuum oven at 80°C for 24 h prior to use.

Preparation of PPC/ALF Composite Films

Five different PPC/ALF composites with PPC/ALF weight ratios of 100/0, 99/1, 97/3, 95/5, 93/7 were prepared in a Hakke Rheomix-600 internal mixer with two roller rotors at 170°C and a rotary speed of 50 rpm for 6 min. The pure PPC was also mixed in the same conditions for comparison. The chamber volume was 50 cm^3 and 50 g materials in total were fed into the mixer for each sample. The PPC/ALF composites were compressed into sheets of 0.5 mm and 1 mm thick at 170°C and 10 MPa for 5 min, respectively. All the films were stored in a desiccator at room temperature for additional testing.

Scanning Electron Microscope

Specimens were prepared by fracturing the films in liquid nitrogen and the morphology of the fractured surfaces were observed with a scanning electron microscope (SEM; Jeol JSM-6330F). Prior to examination, the fractured surfaces were coated with a thin layer of gold.

Tensile Strength Tests

The sheets of 1 mm were cut into dumb-bell shape with dimension of 25 × 4 × 1 mm^3 for static tensile test using a CMT-4104 tensile tester (SANS, Shenzhen, China). The tensile tests were performed at 25°C with a relative humidity of 50 ± 5%. The crosshead speed was set at 50 mm/min and average value of five specimens of every sample was recorded. Moreover, in order to eliminate the influence of temperature and

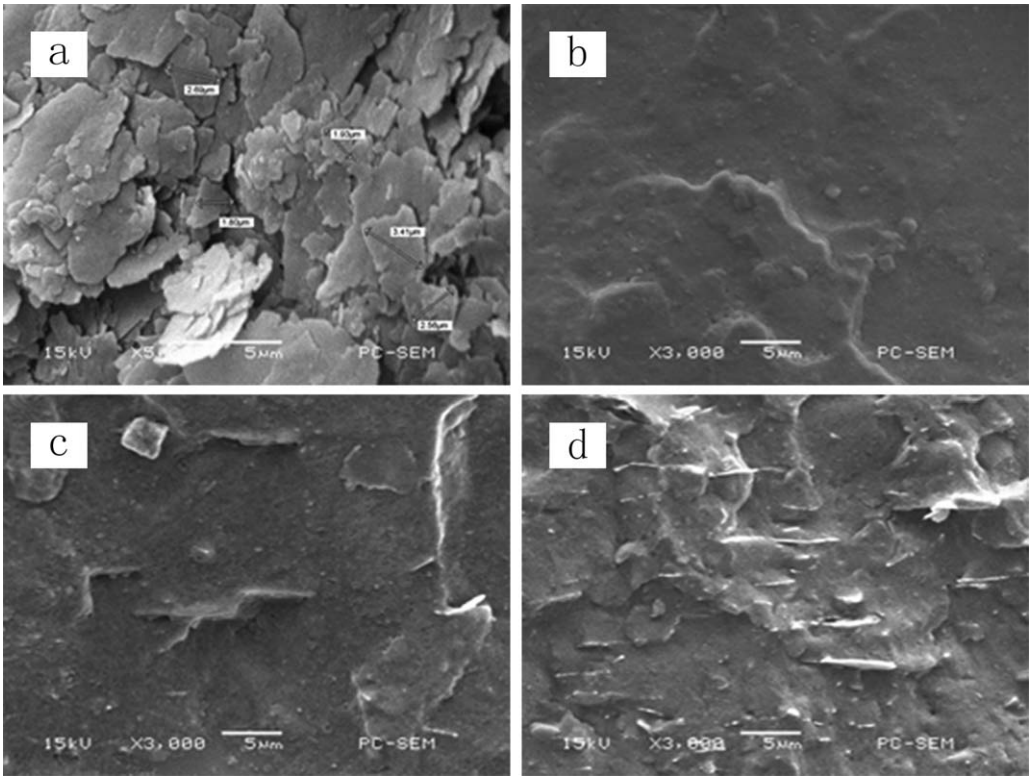

Figure 2. SEM images of ALF and PPC/ALF composite films: (a) ALF; (b) pure PPC; (c) PPC/ALF3 wt %; (d) PPC/ALF7 wt %.

Table I. Tensile Strength of the PPC/ALF Composite Films

Sample	Tensile strength (MPa)	Elongation at break (%)
PPC	12.2 ± 0.4	699 ± 5
PPC/1%ALF	14.2 ± 0.5	619 ± 5
PPC/3%ALF	14.3 ± 0.2	610 ± 6
PPC/5%ALF	17.4 ± 0.4	594 ± 8
PPC/7%ALF	20.7 ± 0.3	512 ± 5

humidity before they were tested, all samples were put in the same conditions.

Differential Scanning Calorimetry Investigation

Glass transition temperatures (T_g) of the samples were measured with differential scanning calorimetry (DSC; Netzsch 204, Burlington, Germany). About 10 mg of each sample was heated from 25°C to 150°C at a rate of 10 °C/min in the first scan and then was cooled to −25°C at a rate of 10 °C/min, after that the second heating scan was performed in the same way as the first. T_g was taken from midpoint of the heat capacity change with temperature of the second scan curve. All the scanning processes were performed under a protective atmosphere of N_2.

Thermogravimetric Analyses

The thermal properties of the composites are measured with a Perkin–Elmer thermogravimetric analysis (TGA)-6 under a nitrogen protective atmosphere. The temperature used ranged from 50 to 500°C with a heating rate of 10°C/min. Prior to the analysis, all the samples were dried in a vacuum oven at 80°C for 24 h.

Water Vapor Transmission Rate

All prepared films were approximately 500 ± 50 μm in thickness. The water vapor transmission rate (WVTR) was measured with "Infrared detection sensor methods," (ISO 15106-2) at 23°C and 85% RH using a WVTR 7500 analyzer (PERMATRAN-W Model 3/61, Mocon, USA). In the testing process, test gas (water vapor) is present in the upper half of the test cell while nitrogen (carrier gas) is routed through the lower half of the test cell. The cell halves are separated by a sample of the material to be tested. Water permeates the material and is picked up by the nitrogen (carrier gas). The nitrogen then exits the cell and passes through the sensor. Mocon WVTR software is used to determine the WVTR. The system provides for a fixed number of test cycles process to determine that the sample has reached equilibrium and the test is complete. And then the water vapor transmission permeation (WVP) is calculated according to the following eq. (1):

Table II. Thermal Properties of the PPC/ALF Composite Films

Sample	T_g (°C)	$T_{-5\%}$ (°C)	T_{max} (°C)
PPC	31.8 ± 0.1	262 ± 1	299 ± 0.5
PPC/1%ALF	31.9 ± 0.1	265 ± 1	300 ± 0.7
PPC/3%ALF	32.5 ± 0.2	267 ± 1	299 ± 0.5
PPC/5%ALF	33.5 ± 0.2	269 ± 1	299 ± 0.6
PPC/7%ALF	34.4 ± 0.1	271 ± 1	299 ± 0.5

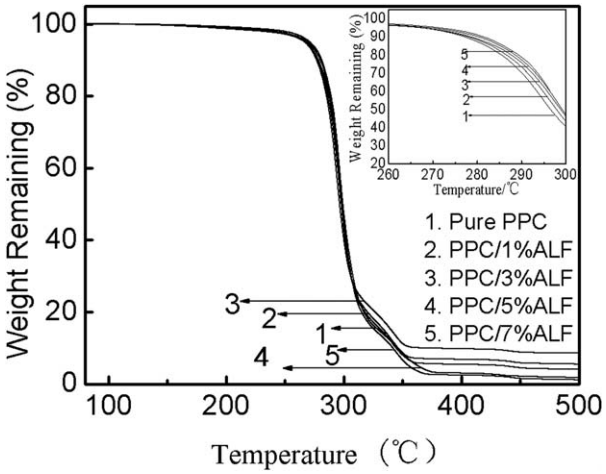

Figure 3. TGA curves of the PPC/ALF composite films.

$$WVP = WVTR \times e \quad (1)$$

where WVP is the water vapor permeability coefficient (g m/(m^2 24 h)), WVTR is the water vapor transmission rate (g/(m^2 24 h)), e is the film thickness (m). The measurements were performed in triplicate.

Oxygen Transmission Rate

The oxygen transmission rate, OTR, was measured according to ASTM D3985-05 using an Y202D oxygen permeation analyzer (GBPI Packing Test Instruments Co., Guangzhou, China). The OTR measurements were performed at a constant temperature of 23°C under dry conditions. Test cells were divided into two chambers separated by the sample. The lower chamber is filled with nitrogen and the upper chamber with oxygen (test gas). Oxygen permeates the material and is picked up by the nitrogen (carrier gas). The nitrogen then exits the cell and passes through the sensor. The amount of oxygen is measured by the sensor to determine the transmission rate (OTR). As the OTR value is relative to both thickness and partial pressure between rich and poor oxygen atmosphere, results were normalized using the following eq. (2):

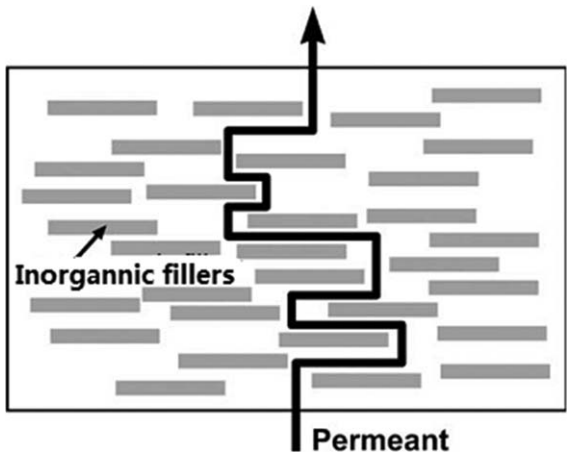

Figure 4. Model for tortuous path of gas through polymer/layered silicate composite (Adapted from Henriette M.C. de Azeredo, 2009[34]).

Table III. OTR, OP, WVTR, and WVP of the PPC/ALF Composite Films

Sample	Thickness (μm)	OTR ($cm^3/(m^2$ 24 h))	OP (cm^3 mm/(m^2 24 h))	WVTR (g/(m^2 24 h))	WVP (g mm/(m^2 24 h))
PPC	485 ± 5	4.60 ± 0.001	2.25 ± 0.004	2.16 ± 0.05	1.05 ± 0.02
PPC/1%ALF	510 ± 5	2.60 ± 0.001	1.31 ± 0.005	2.00 ± 0.05	1.02 ± 0.03
PPC/3%ALF	574 ± 5	1.90 ± 0.001	1.10 ± 0.006	1.60 ± 0.05	0.92 ± 0.03
PPC/5%ALF	563 ± 5	1.30 ± 0.001	0.73 ± 0.006	1.41 ± 0.05	0.79 ± 0.03
PPC/7%ALF	559 ± 5	3.20 ± 0.001	1.82 ± 0.006	1.40 ± 0.05	0.78 ± 0.03

$$\mathrm{OP} = \frac{\mathrm{OTR} \times e}{\Delta p} \quad (2)$$

where OP is the oxygen permeability coefficient (cm^3 m/(m^2 24 h atm)), OTR is the oxygen transmission rate ($cm^3/(m^2$ 24 h)), e is the film thickness (m), and Δp is the oxygen partial pressure difference. In our experiment, the oxygen Δp was 1 atm and all samples were cut into a circular shape of 50 cm^2. Moreover, two films of each sample were tested and the results were averaged.

RESULTS AND DISCUSSION

Morphology of the PPC/ALF Composite Films

The morphological structure of composites is a very important characteristic as it ultimately affects the thermal stability, tensile properties, and water vapor and oxygen permeability of the composites. SEM was used to investigate the morphological structure of PPC/ALF composite films.

As shown in Figure 2(a) aluminum powder is flake structure with average size about 3–5 μm and thickness about 280–340 nm. From morphologies of the cross-section of the PPC/ALF composites, we can see that the ALFs are well dispersed within the composites and oriented parallel to the composites sheet plane. The interface between ALF and PPC is obscure, indicating the good interfacial adhesion between ALF and PPC matrix. However, for the PPC/7%ALF composite, some cracks can be observed at the interface of PPC and ALF. The existence of the cracks might bring negative effect on the tensile and gas barrier properties of the composite films.

Tensile Strength of PPC/ALF Composite Films

The tensile strength (TS) and elongation of five different PPC/ALF composite films were investigated using a temperature-controlled tensile tester, which are summarized in Table I. It is observed that the TS of the PPC/ALF composites are improved by 16, 17, 42, and 69% upon the incorporation of 1, 3, 5, and 7% wt ALF in turn. The increase in the TS of PPC/ALF films with the addition of ALF is a typical effect of inorganic fillers on polymer matrix.[28] It is supposed that the incorporation of platelet fillers, such as ALF, into PPC matrix leads to better stress transferability and therefore enhances the TS of the composites.[29]

From a structural point of view, PPC can be described as a ductile and flexible polymer at room temperature owing to the combination of aliphatic propylene linkage and flexible carbonate linkage in the repeated unit, while the ALF particle is rigid filler. Therefore, the incorporation of ALF can result in a sharp elongation reduction for these composite films. However, from Table I, we observe that elongation at break of the PPC/ALF composites decrease gradually with increasing ALF contents. The elongation of pure PPC is 699% while the PPC/7 wt %ALF composite film still has high elongation value of 512%. It is interesting that there is no significant change in elongation when the ALF is added. This phenomenon can be attributed to the high aspect ratio of the ALF and the good adhesion better between PPC and ALF. In short, the incorporation of ALF leads to improvement in the tensile properties of the composites from the fact that the TS is greatly increased while the elongation at break is only slightly decreased.

Thermal Properties of the PPC/ALF Composite Films

In general, the incorporation of inorganic fillers, especially high aspect ratio fillers, into polymers can enhance thermal properties.[30,31] DSC and TGA were performed to investigate how the ALF particles affect the thermal properties of PPC/ALF composite films. Glass transition temperatures (T_gs) of PPC/ALF composite films derived from the DSC curves are summarized in Table II. T_g of neat PPC is 31.9°C, and the T_g values of PPC/ALF composite films increase with increasing ALF contents. The PPC/7%ALF composite exhibits a T_g of 34.4°C. The increase of T_g of PPC by incorporating ALF is attributed to the hindering of the movement of PPC chain by ALF. However, this hindering effect is observed in a very limited scale indicating that the interfacial interaction between PPC and ALF is not very strong. This is because there is no functional group on the surface of ALF that can interact with PPC molecules.

The thermal degradation curves of pure PPC and PPC/ALF composites are shown in Figure 3 and the −5% and maximum weight loss temperatures ($T_{-5\%}$ and T_{max}) are summarized in Table II. As shown in Figure 3, all the samples show a two-stage degradation process. In the first stage, an obvious weight loss occurred at around 250–310°C corresponding to the structural decomposition of the polymers. As for the second stage, at about 300–400°C, the weight loss is attributed to the further decomposition of PPC residual. It is obvious that all samples exhibit similar thermal degradation behavior, which indicates the introduction of ALF does not significantly affect the thermal degradation patterns of PPC/ALF composite films. As summarized in Table II, the degradation temperatures ($T_{-5\%}$) of PPC/ALF composites are higher than that of pure PPC and increases with increasing ALF contents due to the shielding effect of the ALF particles.

Barrier Properties of the PPC/ALF Composite Films

Good oxygen and water vapor barrier properties are essential for obtaining a long protective period for packaged products.[32,33]

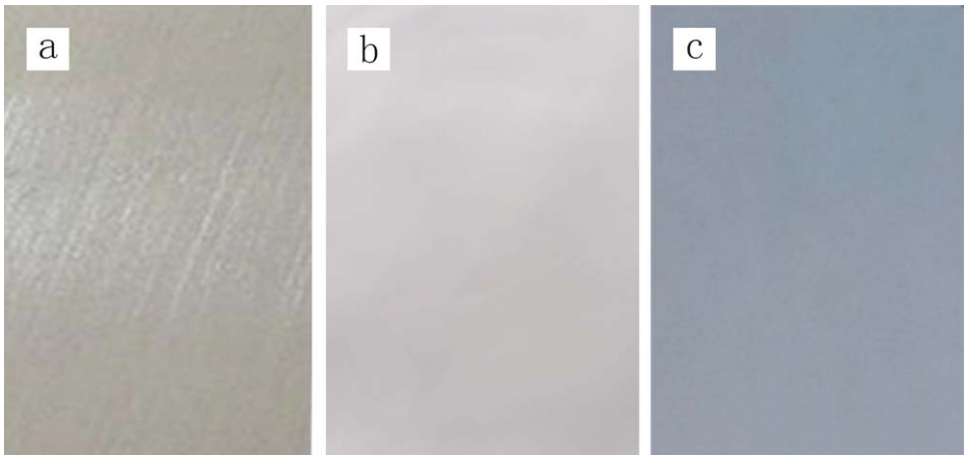

Figure 5. Images of (a) aluminum sheet; (b) PPC/3% wt ALF; (c) neat PPC. [Color figure can be viewed in the online issue, which is available at wileyonlinelibrary.com.]

Internal damage could be suppressed and long-term performance could be enhanced by the reduction of oxygen and water transmission. Thus, barrier films have to prevent or at least decline the oxygen and water transfer between the product and the surrounding atmosphere. Layered inorganic particles are considered impenetrable by gas molecules. Therefore, it is believed that the addition of layered inorganic particles in the polymeric matrix would improve its barrier properties by lengthening a bypass path of gas as they diffuse through the material, decelerating the process of the penetration (Figure 4).[34,35] This phenomenon has been observed in many polymer/layered silicate composites.[36,37] From morphologies of the cross-section of the PPC/ALF composites (Figure 2), we can see that the ALFs are well dispersed within the composites and oriented parallel to the composites sheet plane. The oriented parallel structure of ALFs is formed during the melt mold compress because of both viscous melt flow of polymer matrix and thin film produced. The special structure can also be controlled and formed using other melt process method like melt extruding.

In this study, the OTR and WVTR of the PPC/ALF composite films were investigated to evaluate the enhancement effect of ALF filling on the oxygen and water barrier properties of PPC. The results are listed in Table III. The oxygen permeability coefficient (OP) and water vapor permeability coefficient (WVP) are calculated from the measured OTR and WVTR values. It is obvious that both OP and WVP of the PPC/ALF composites decrease with increasing ALF contents. The OP and WVP of the PPC/ALF composite film with 5 wt % ALF are 32.4% and 75.2% respectively that of pure PPC. The apparent alleviation of oxygen and water vapor molecular diffusion by the introduction of ALF particles can be attributed to the oriented dispersion of the ALF within PPC matrix, which can effectively lengthen a bypass path of gas molecular. However, the oxygen transmission increases when continuing adding ALF loading level up to 7 wt %, this could be due to the aggregation of ALF and some cracks emerging at the interface between PPC matrix and ALF particles as evidenced by SEM.

Table IV. Gas Barrier Properties of Some Polymer Films Used in Flexible Packaging Applications

Sample	OP (cm^3 mm/(m^2 24 h))	WVP (g mm/(m^2 24 h))
PPC	2.25	1.05
PPC/3%ALF	1.10	0.92
PE	50–200	0.5–2
PA	1.41	0.5–10

As shown in Figure 5, the PPC/3%ALF composite film exhibits metallic luster, which is similar to aluminum sheet. Additionally, the oxygen and water vapor permeability of PPC/3%ALF composite film is lower than that of PA6 (Table IV).[38] This implies that PPC/ALF composites have competitive potential as packaging polymeric materials. Besides, the gas barrier properties of PPC/3%ALF is better than PE together with its totally biodegradable nature.[39]

CONCLUSIONS

In terms of oxygen and moisture barrier properties of PPC/ALF composite films, the oxygen and water permeation process put forward an important barrier improvement, which is due to the increase of the tortuous diffusion pathways induced by impermeable aluminum flake within PPC matrix. Meanwhile, the TS considerably increases, while the elongation at break only marginally decreases owing to the incorporation of ALF. It can be concluded that the addition of ALF platelet fillers into polymers can obviously enhance the tensile properties of PPC matrix. Similarly, the incorporation of ALF can also improve the thermal properties of PPC. Therefore, the PPC/ALF composite films show potential application as packaging polymeric materials.

ACKNOWLEDGMENTS

The authors would like to thank the National Natural Science Foundation of China (Grant No. 21376276), the Special-funded Program on National Key Scientific Instruments and Equipment Development of China (Grant No. 2012YQ230043), Guangdong Province Universities and Colleges Pearl River Scholar Funded

Scheme (2010), Guangdong Province Sci & Tech Bureau (Key Strategic Project Grant No. 2008A080800024), Special Projects on the Integration of Industry, Education and Research of Guangdong Province, and the Fundamental Research Funds for the Central Universities for financial support for this work.

REFERENCES

1. Inoue, Y.; Yoshie, N. *Prog. Polym. Sci.* **1992**, *17*, 571.
2. Okada, M. *Prog. Polym. Sci.* **2002**, *27*, 87.
3. Broecker, W. S. *Science* **1997**, *278*, 1582.
4. Meehl, G. A. *Nature* **1996**, *382*, 56.
5. Kacholia, K.; Reck, R. A. *Climate Change* **1997**, *35*, 53.
6. Inoue, S.; Koinuma, H.; Tsuruta, T. *Makromol. Chem.* **1969**, *130*, 210.
7. Zhu, Q.; Meng, Y. Z.; Tjong, S. C.; Zhao, X. S; Chen, Y. L. *Polym. Int.* **2002**, *51*, 1079.
8. Yu, Z.; Xu, L.; Wei, Y.; Wang, Y.; He, Y.; Xia, Q. *Chem. Commun.* **2009**, 3934.
9. Zhu, Q.; Meng, Y. Z.; Tjong, S. C.; Zhang, Y. M.; Wan, W. *Polym. Int.* **2003**, *52*, 799.
10. Li, X. H.; Tjong, S. C.; Meng, Y. Z.; Zhu, Q. *J. Polym. Sci. Part B: Polym. Phys.* **2003**, *41*, 1806.
11. Ge, X. C.; Xu, Y.; Meng, Y. Z.; Li, R. K. Y. *Compos. Sci. Technol.* **2005**, *65*, 2219.
12. Qin, Y. S.; Wang, X. H.; Zhang, S. B.; Zhao, X. J.; Wang, F. S. *J. Polym. Sci. Part A: Polym. Chem.* **2008**, *46*, 5959.
13. Chisholm, M. H.; Navarro-Liobet, D.; Zhou, Z. P. *Macromolecules* **2002**, *35*, 6494.
14. Sugimoto, H.; Inoue, S. *Pure Appl. Chem.* **2008**, *78*, 1823.
15. Wang, S. J.; Tjong, S. C.; Du, L. C.; Zhao, X. S.; Meng, Y. Z. *J. Appl. Polym. Sci.* **2002**, *85*, 2327.
16. Zhu, Q.; Meng, Y. Z.; Tjong, S. C.; Zhao, X. S.; Chen, Y. L. *Polym. Int.* **2009**, *51*, 1079.
17. Yunho, L.; Dowan, K.; Jongchul, S.; Haksoo, H.; Sher, B. K. *Polym. Int.* **2013**, *62*, 1386.
18. Peng, S.; An, Y.; Chen, C.; Fei, B.; Zhuang, Y.; Dong, L. *Polym. Degrad. Stab.* **2003**, *80*, 141.
19. Ma, X.; Chang, P. R.; Yu, J.; Wang, N. *Carbohydr. Polym.* **2008**, *71*, 229.
20. Zhang, Z.; Zhang, H.; Zhang, Q.; Zhou, Q.; Zhang, H.; Mo, Z. *J. Appl. Polym. Sci.* **2006**, *100*, 584.
21. Shi, X.; Gan, Z. *Eur. Polym. J.* **2007**, *43*, 4852.
22. Seo, J.; Jeon, K.; Jang, E.; Han, H. *J. Appl. Polym. Sci.* **2011**, *122*, 1101.
23. Tsuji, H.; Kawashima, Y.; Takikawa, H.; Tanaka, S. *Polymer* **2007**, *48*, 4213.
24. Koros, W. Barrier polymers and structures; J. American Chemical Society: Washington, D.C., **1990**; Vol. *26*, p 225.
25. Sekelik, D. J.; Stepanov, E. V.; Nazarenko, S.; Schiraldi, D.; Hiltner, A.; Baer, E. *J. Appl. Polym. Sci.* **1999**, *37*, 847.
26. Benmalek, M.; Dunlop, H. M. *Surf. Coat. Technol.* **1995**, *76–77*, 821.
27. Chatham, H. *Surf. Coat. Technol.* **1996**, *78*, 1.
28. Murthy, N. S.; Kotliar, A. M.; Sibilia, J. P.; Sacks, W. *J. Appl. Polym. Sci.* **1986**, *31*, 2569.
29. Whaling, A.; Bhardwaj, R.; Mohanty, A. K. *Ind. Eng. Chem. Res.* **2006**, *45*, 7497.
30. Ramanthan, T.; Abdala, A. A.; Stankovich, S.; Dikin, D. A.; Herrera-Alonso, M.; Piner, R. D.; Admson, D. H.; Schniepp, H. C.; Chen, X.; Ruoff, R. S.; Nguyen, S. T.; Aksay, I. A.; Prud'homme, R. K.; Brinson, L. C. *Nat. Nanotechnol.* **2008**, *3*, 327.
31. Wang, J. C.; Wang, X. B.; Xu, C. H.; Zhang, M.; Shang, X. P. *Polym. Int.* **2011**, *60*, 816.
32. Yu, J.; Yang, J.; Liu, B.; Ma, X. *Bioresour. Technol.* **2009**, *100*, 2832.
33. Bajpai, S. K.; Chand, N.; Chaurasia, V. *J. Appl. Polym. Sci.* **2010**, *115*, 674.
34. Hernandez, R. J.; Selke, S. E. M.; Culter, J. D. *Plast. Packaging* **2000**, *109*, 299.
35. Sun, L. Y.; Boo, W.-J.; Clearfield, A.; Sue, H.-J.; Pham, H. Q. *J. Membr. Sci.* **2008**, *318*, 129.
36. Azeredo, H. M. C. *Food Res. Int.* **2009**, *42*, 1240.
37. Ray, S.; Yamada, K.; Okamoto, M.; Ogami, A.; Ueda, K. *Chem. Mater.* **2003**, *15*, 2289.
38. Alix, S.; Follain, N.; Tenn, N.; Alexandre, B. *J. Phys. Chem. C.* **2012**, *116*, 4937.
39. Lange, J.; Yves, W. *Package. Technol. Sci.* **2003**, *16*, 149.